

Preparation and properties of surface textured ZnO:Al films by direct current pulse magnetron sputtering

Ying Wang · Hualin Wang · Yun Wang ·
Wanyu Ding · Shou Peng · Weiping Chai

Received: 22 June 2012 / Accepted: 7 July 2012 / Published online: 15 July 2012
© Springer Science+Business Media, LLC 2012

Abstract Transparent conductive surface textured Al-doped zinc oxide (ZnO:Al, AZO) thin films were prepared on glass substrates by direct current pulse magnetron sputtering at substrate temperature of 270 °C and post-etching in NaOH solution at room temperature. The effects of Ar flow rate on the structural, optical, electrical properties and light trapping ability were investigated systematically. With the increasing of Ar flow rate from 10 to 50 sccm, different surface features ranging from honeycomb-like to crater-like structures were observed. The relationship between surface textured structures and Ar flow rate was discussed. The AZO film deposited with Ar flow rate in 50 sccm displayed fine optoelectronic properties, improved figure of merit and effective surface textured structures for light trapping, which could be applied as a transparent conducting electrode in silicon-based thin film solar cells.

1 Introduction

Aluminum doped zinc oxide (ZnO:Al, AZO), a promising transparent conducting oxide material, has been widely

used as transparent electrode for optoelectronic devices [1–4]. Specifically, as standard front contacts, AZO films have received great interest in the applications of silicon-based thin film solar cells, owing to their high transparency in the visible wavelength range and low resistivity, as well as their low cost, non-toxicity and stability under hydrogen plasma environment [5–7]. In addition, textured surfaces of AZO films are required to provide the effective light trapping, which can elongate the effective light path. Therefore, surface morphology is an important characteristic for surface textured AZO films to realize light scattering. Compared with smooth AZO films, surface textured AZO films could improve the short circuit current and the conversion efficiency [8, 9]. Textured surface can be realized by wet chemical etching after sputtering deposition of AZO films. In most researches, typical acid used for the surface textured AZO process is hydrochloric acid (HCl) solution at a concentration of 0.5 % [10–12]. However, it is difficult for HCl solution to control the etching process and surface morphology of AZO films because of the high etching rate of HCl solution. Therefore, to slow down the etching rate, NH₄Cl solution and weak acetic acid solution were used as etchant, but the surface morphology was not quite satisfactory yet [13, 14]. NaOH solution can also be an alternative etchant to obtain surface textured AZO films, which can control the etching process and the surface morphology effectively [15]. But up to now, few studies on the surface textured AZO films etched with NaOH solution have been reported systematically.

The growth and etching process of sputtered AZO films are influenced by deposition conditions such as substrate temperature, working pressure and Ar flow rate. Up to now, the studies on detailed and sufficient etching mechanism and model are underway. Hence, to achieve appropriate features for light scattering, it is necessary to study the

Y. Wang (✉) · H. Wang · W. Ding · W. Chai
School of Materials Science and Engineering, Dalian Jiaotong
University, Dalian 116028, China
e-mail: djtuwy@163.com

Y. Wang · H. Wang · W. Ding · W. Chai
Engineering Research Center of Optoelectronic Materials
and Devices, Education Department of Liaoning Province,
Dalian 116028, China

Y. Wang · S. Peng
State Key Laboratory of Advanced Technology for Float Glass,
Bengbu 233018, China

influence of deposition conditions on the surface morphology and the etching behavior. In this paper, we prepared surface textured AZO thin films by direct current pulse magnetron sputtering and post-etching in NaOH solution. The influence of Ar flow rate on the structural, optical, electrical properties, light trapping ability and etching behavior was investigated in detail.

2 Experimental

AZO films with 700 nm in thickness were prepared on glass substrates by direct current pulse magnetron sputtering at substrate temperature of 270 °C. A ceramic ZnO:Al₂O₃ (98 wt%:2 wt%) target was used. Before the AZO films were deposited, the glass substrates were cleaned and loaded into the sputtering chamber. The base pressure was operated at 3×10^{-3} Pa. Then Ar (99.999 % in purity) was introduced into the chamber as sputtering gas. Deposition was carried out after pre-sputtering for 5 min in order to clean the target surface. During the process of deposition, Ar flow rate was varied from 10 to 50 sccm, with 10 sccm in step. The other deposition conditions were kept constant. The working pressure and the sputtering power were 0.8 Pa and 350 W, respectively. After the sputtering deposition, all the AZO films were immersed in 5 wt% NaOH solution etching for 30 min to obtain the textured surface at room temperature.

The crystal structure of the AZO films was analyzed by X-ray diffraction (XRD) using a PANalytical X'pert diffractometer with Cu radiation. The surface morphology of the AZO films was observed by JEOL JSM-6360LV scanning electron microscopy (SEM). Optical properties of the AZO films were performed using a U-3310 ultraviolet-visible spectrophotometer with an integrating sphere. The electrical properties were measured at room temperature by a Loresta EP MCP-T360 four-point probe.

3 Results and discussion

3.1 Structural properties

The XRD patterns of AZO films deposited with different Ar flow rates are shown in Fig. 1. All the films show a strong diffraction peak located at 2θ of 34.2° and a weak peak at 72.2°, which correspond to the (002) and (004) peak, respectively. It indicates that all the AZO thin films have a polycrystalline hexagonal wurtzite structure with a c-axis preferred orientation [16]. The results reveal that the dopant Al does not change the hexagonal wurtzite structure in the AZO film. And no characteristic peaks related to Al₂O₃ phase are found. Besides, the position of the (002) and (004) peak do not shift significantly as increasing the Ar flow rate.

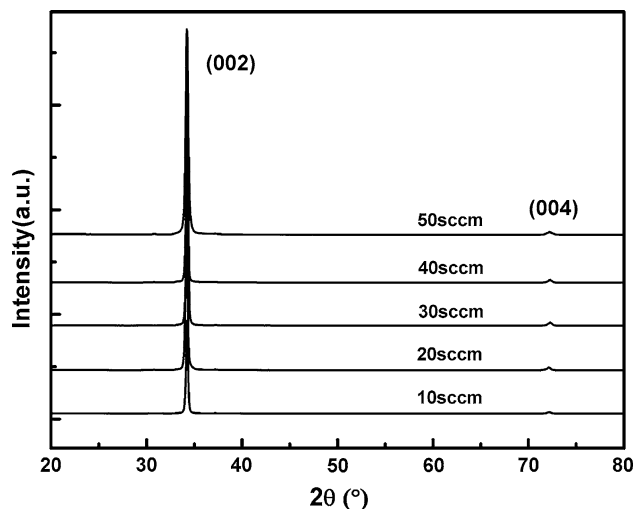


Fig. 1 XRD patterns of AZO films deposited under different Ar flow rates

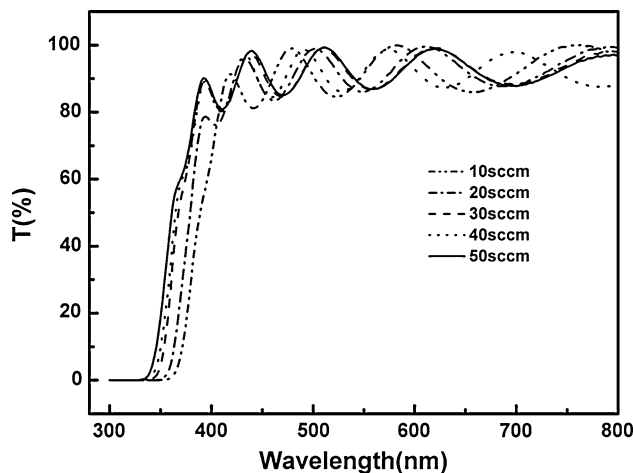


Fig. 2 Optical transmittance spectra of AZO films under different Ar flow rates

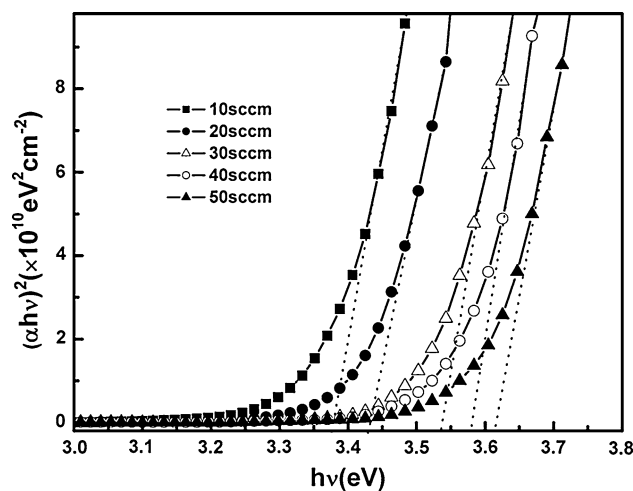


Fig. 3 Optical band gap of AZO films under different Ar flow rates

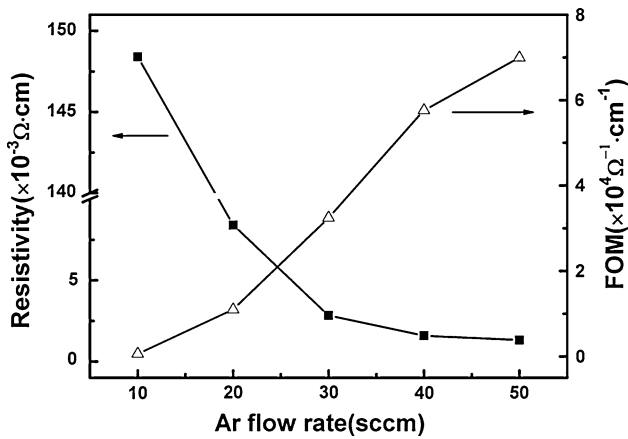


Fig. 4 Resistivity and FOM of AZO films as a function of Ar flow rate

3.2 Optical and electrical properties

The dependence of optical properties on Ar flow rate is investigated. Fig. 2 shows the transmittance spectra with different Ar flow rates. As for photovoltaic applications, the high optical transmittance in the visible region is essential for AZO films. From Fig. 2, high transparency is observed throughout the visible wavelength range with an average transmittance of above 90 % for all AZO films. In the UV region, all the films exhibit a sharp fundamental absorption edge. With increasing the Ar flow rate, the absorption edge shifts monotonically to the shorter wavelength, which is a consequence of increased optical band gap.

Based on the measured transmittance spectra, we plot the $(\alpha h\nu)^2$ curves as a function of $h\nu$ for AZO films

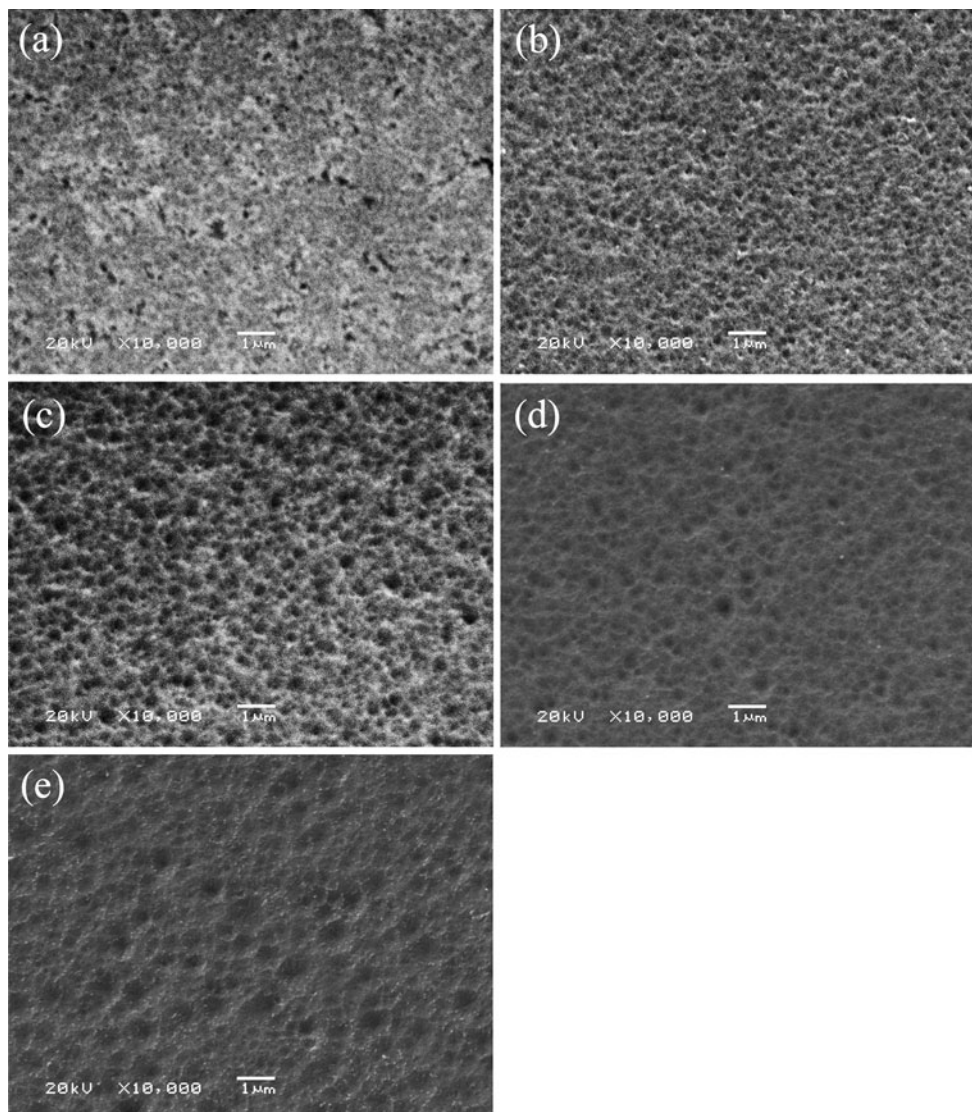


Fig. 5 SEM micrographs of the etched AZO films deposited under different Ar flow rates: a 10 sccm, b 20 sccm, c 30 sccm, d 40 sccm, e 50 sccm

deposited with different Ar flow rates, as shown in Fig. 3. As a direct band gap semiconductor, the optical band gap (E_g) of the AZO films can be determined by the extrapolation methods from $(\alpha hv)^2 = A(hv - E_g)$, where α is the absorption coefficient, hv is the photon energy, and A is a constant for direct transition, respectively [17]. As we can see from Fig. 3, E_g remarkably increases from 3.38 to 3.61 eV as Ar flow rate increases from 10 to 50 sccm, which is due to Burstein–Moss effect. Compared with pure ZnO films, Al doping will result in a widening of the band gap. And the energy shift ΔE_g is proportional to $n^{3/2}$, where n is the carrier concentration [18, 19]. So with increasing the Ar flow rate, the blue shift is caused by the increasing of carrier concentration.

Figure 4 shows the resistivity and the figure of merit (FOM) of AZO films as a function of Ar flow rate. It can be seen that the resistivity of the deposited AZO films shows a decreasing from 0.148 Ω cm to 1.3×10^{-3} Ω cm. This is attributed to the residual oxygen in the chamber. Higher residual oxygen content under lower Ar flow rate in the sputtering gas will increase the absorbed oxygen stacked at the grain boundaries, which acts as the electron trap and causes the decreasing of the carrier concentration. This corresponds well with the optical measurements of AZO films with various Ar flow rates mentioned above. On the other hand, the absorbed oxygen could give rise to the band bending and therefore result in the barrier at the grain boundaries [20]. Under lower Ar flow rate, much more absorbed oxygen raises the barrier and then reduces the mobility. Thus, the resistivity is higher under lower Ar flow rate. The FOM, which is the ratio of the average transmittance in the visible wavelength range to the resistivity, can be used to estimate the performance of the AZO films. With increasing the Ar flow rate, the FOM of AZO films increases. The highest FOM value is 7×10^4 Ω^{-1} cm $^{-1}$ with Ar flow rate in 50 sccm, which is suitable for AZO films as the transparent front contacts applied in silicon-based thin film solar cells.

3.3 Textured surface morphology

The control of surface morphology is important for the surface textured AZO films and influences the light trapping ability greatly. SEM micrographs of etched AZO films deposited with different Ar flow rates are shown in Fig. 5. Obvious different surface features, ranging from honeycomb-like to crater-like structures, reveal the effect of Ar flow rate on etching behavior. For polycrystalline AZO films, every grain boundary has a potential for etching, which depends on the compactness of the grain boundary [21]. The etching might start at less order and less compact grain boundaries, which have higher potentials for etching,

and then develop the vertical and horizontal etching process at the grain boundaries.

As mentioned above, more oxygen adsorbed at the gain boundaries under lower Ar flow rate results in the changes of optoelectronic properties for AZO films. Meanwhile, more adsorbed oxygen could make less order grain boundaries which are more easily attacked by the etchant. Under lower Ar flow rate, more disorder grain boundaries may cause a honeycomb-like structure. As we can see that when the Ar flow rate reaches at 50 sccm, the surface of AZO film is almost uniformly covered by the discernable craters with diameters ranging from 0.5 to 1 μ m, which is an effective feature for light scattering.

3.4 Light trapping ability

Besides the surface morphology, the haze which is defined as the ratio of diffuse to total transmittance ($H = T_{\text{diff}}/T_{\text{total}}$) is another important indicator of the light trapping ability for surface textured AZO films. High haze value implies a good light trapping ability. The haze of the surface textured AZO films as a function of Ar flow rate is studied and shown in Fig. 6. The haze value at the 550 nm wavelength increases with increasing the Ar flow rate monotonically. This means that the light scattering is more obvious and the light trapping ability becomes better. Maximum haze value at the wavelength of 550 nm is achieved for surface textured AZO film deposited under the Ar flow rate in 50 sccm. The relationship between spectral haze and Ar flow rate is well coherent to the results of the observed surface morphology by SEM measurements.

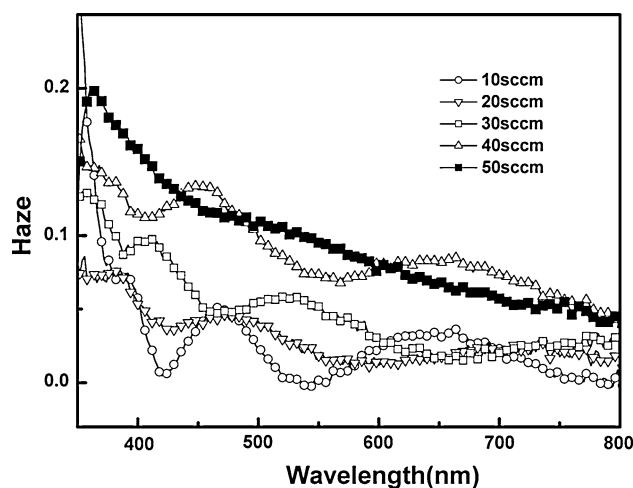


Fig. 6 Haze spectra of surface textured AZO films as a function of Ar flow rate

4 Conclusions

AZO films were prepared on glass substrates by direct current pulse magnetron sputtering at 270 °C and 5 wt% NaOH solution was used to obtain the textured surface at room temperature. All the AZO thin films showed a hexagonal wurtzite structure with a c-axis preferred orientation. The increasing of Ar flow rate resulted in the reducing of the resistivity, widening of the band gap and improving of the figure of merit. Surface features changed from honeycomb-like to crater-like structures with increasing the Ar flow rate. And typical effective crater-like textured structures were observed under Ar flow rate in 50 sccm. Surface textured AZO thin films etched with NaOH solution have satisfactory optoelectronic properties and good light trapping ability, which is suitable for applications as transparent contacts in silicon-based thin film solar cells.

Acknowledgments This work was supported by the National Natural Science Foundations of China (Grant No. 51002018 and 51102030), the Project of Open Research Foundation of the Ministry of Education Key Laboratory of Materials Modification (Dalian University of Technology) (Grant No. DP1050901), the Program for Liaoning Excellent Talents in University (Grant No. LJQ2011043), the Dalian Economy and Communication Committee Foundation of China (Grant No. 2009-3-215-jw-cxyhz) and the Dalian Science and Technology Plan Projects of China (Grant No. 2010J21DW008 and 2011A15GX025).

References

- S. Yodyingyong, Q.F. Zhang, K. Park, C.S. Dandeneau, X.Y. Zhou, D. Triampo, G.Z. Cao, *Appl. Phys. Lett.* **96**, 073115 (2010)
- A. Boukhachem, B. Ouni, M. Karyaoui, A. Madani, R. Chtourou, M. Amlouk, *Mater. Sci. Semicond. Process.* **15**, 282 (2012)
- X.J. Wang, X.B. Zeng, D.Q. Huang, X. Zhang, Q. Li, *J. Mater. Sci. Mater. Electron.* (2012). doi:10.1007/s10854-012-0632-x
- B.J. Babu, A. Maldonado, S. Velumani, R. Asomoza, *Mater. Sci. Eng. B* **174**, 31 (2010)
- Y.H. Kim, K.S. Lee, T.S. Lee, B.K. Cheong, T.Y. Seong, W.M. Kim, *Curr. Appl. Phys.* **10**, S278 (2010)
- B.S. Chua, S. Xu, Y.P. Ren, Q.J. Cheng, K. Ostrikov, *J. Alloys Compd.* **485**, 379 (2009)
- Y.C. Lin, Y.C. Jian, J.H. Jiang, *Appl. Surf. Sci.* **254**, 2671 (2008)
- H. Zhu, J. Hüpkes, E. Bunte, S.M. Huang, *Surf. Coat. Technol.* **205**, 773 (2010)
- S.J. Tark, M.G. Kang, S. Park, J.H. Jang, J.C. Lee, W.M. Kim, J.S. Lee, D. Kim, *Curr. Appl. Phys.* **9**, 1318 (2009)
- M. Berginski, J. Hüpkes, A. Gordijn, W. Reetz, T. Wätjen, B. Rech, M. Wuttig, *Sol. Energy Mater. Sol. Cells* **92**, 1037 (2008)
- T. Tohsophon, J. Hüpkes, H. Siekmann, B. Rech, M. Schultheis, N. Sirikulrat, *Thin Solid Films* **516**, 4628 (2008)
- M. Wimmer, F. Ruske, S. Scherf, B. Rech, *Thin Solid Films* **520**, 4203 (2012)
- X.J. Wang, H. Wang, W.L. Zhou, G.X. Li, J.Yu, *Mater. Lett.* **65**, 2039 (2011)
- X.Y. Gao, Q.G. Lin, H.L. Feng, Y.S. Chen, S. Yang, J.H. Gu, W.Q. Li, J.X. Lu, *Appl. Surf. Sci.* **255**, 7268 (2009)
- Y. Wang, Y.S. Gu, S. Peng, W.Y. Ding, H.L. Wang, W.P. Chai, *Appl. Surf. Sci.* **257**, 8044 (2011)
- S. Singh, R.S. Srinivasa, S.S. Major, *Thin Solid Films* **515**, 8718 (2007)
- J. Tauc, R. Grigorovici, A. Vancu, *Phys. Stat. Sol.* **15**, 627 (1966)
- F. Urbach, *Phys. Rev.* **92**, 1324 (1953)
- R. Cebulla, R. Wendt, K. Ellmer, *J. Appl. Phys.* **83**, 1087 (1998)
- J.W. Orton, M.J. Powell, *Rep Prog Phys* **43**, 1263 (1980)
- J. Hüpkes, J.I. Owen, S.E. Pust, E. Bunte, *Chem Phys Chem* **13**, 66 (2012)